

From Models to Network Topologies: A Topology Inference Attack in Decentralized Federated Learning

Chao Feng¹, Yuanzhe Gao¹, Alberto Huertas Celdrán¹, G r me Bovet², Burkhard Stiller¹

¹Communication Systems Group, Department of Informatics, University of Z rich, Binzm hlestrasse 14, CH-8050 Z rich, Switzerland

²Cyber-Defence Campus, armasuisse Science & Technology, CH-3602 Thun, Switzerland
{cfeng, huertas, stiller}@ifi.uzh.ch, yuanzhe.gao@uzh.ch, gerome.bovet@armasuisse.ch

Abstract

Federated Learning (FL) is widely recognized as a privacy-preserving machine learning paradigm due to its model-sharing mechanism that avoids direct data exchange. However, model training inevitably leaves exploitable traces that can be used to infer sensitive information. In Decentralized FL (DFL), the overlay topology significantly influences its models' convergence, robustness, and security. This study explores the feasibility of inferring the overlay topology of DFL systems based solely on model behavior, introducing a novel Topology Inference Attack. A taxonomy of topology inference attacks is proposed, categorizing them by the attacker's capabilities and knowledge. Practical attack strategies are developed for different scenarios, and quantitative experiments are conducted to identify key factors influencing the attack effectiveness. Experimental results demonstrate that analyzing only the public models of individual nodes can accurately infer the DFL topology, underscoring the risk of sensitive information leakage in DFL systems. This finding offers valuable insights for improving privacy preservation in decentralized learning environments.

1 Introduction

Federated Learning (FL) has emerged as a novel framework for enabling privacy-preserving Machine Learning (ML), facilitating collaborative model training among distributed clients without the necessity of sharing raw data [McMahan *et al.*, 2017]. Conventional FL systems are predicated on a centralized architecture, referred to as Centralized FL (CFL), wherein a central entity is responsible for collecting, aggregating, and redistributing models to the clients. Nevertheless, this centralized architecture presents several challenges, such as processing bottlenecks and the single points of failure risk [Beltr n *et al.*, 2023]. In response to these limitations, Decentralized FL (DFL) has been introduced, wherein model training and aggregation occur locally, and communication between nodes relies on P2P networks peer-to-peer (P2P) network. This approach eliminates dependency on a

central server, mitigating risks associated with single points of failure [Beltr n *et al.*, 2024].

Although FL, both centralized and decentralized, protect raw data privacy through its unique model-sharing mechanism, the training process inevitably leaves traces in the models. These traces may be susceptible to exploitation by malicious actors, potentially leading to inference attacks, including membership inference attacks, property inference attacks, and attribute inference attacks [Hu *et al.*, 2022]. Previous studies have illustrated that such attacks pose a considerable risk to privacy within FL systems by elucidating sensitive information based on the behavior of the models [Dayal *et al.*, 2023]. While much of the existing work focuses on the CFL, a notable research gap exists in exploring information leakage risks associated with DFL.

Overlay network topology defines how participants are interconnected in an FL system. In CFL, the client-server architecture enforces a fixed, star-shaped topology. However, DFL leverages the P2P network, enabling flexible node connections to form diverse topologies. Existing studies demonstrate that topology significantly influences DFL models' robustness and privacy-preserving capabilities [Feng *et al.*, 2024]. Thus, topology should be considered sensitive data and a critical asset within DFL systems. However, theoretical analyses on how network topology affects model convergence remain sparse. Moreover, there is limited research investigating potential information leakage risks for this sensitive overlay topology data and strategies to safeguard this critical asset.

This paper addresses this research gap by proposing a novel overlay topology inference attack targeting DFL systems. The proposed attack leverages the behavioral traces generated by models to uncover sensitive overlay topologies. The main contributions of this work are as follows: (i) the formulation of a taxonomy of topology inference attacks, classifying these attacks based on the attacker's capabilities and knowledge; (ii) the development of practical strategies tailored to various attack types, accompanied by a quantitative analysis of critical factors that influence the efficiency of these attacks; (iii) rigorous experimental evaluations conducted across a range of datasets and topology configurations to empirically validate the proposed attack strategies; and (iv) the provision of insights aimed at informing the design of effective defensive mechanisms to safeguard sensitive information and preserve privacy within DFL systems.

2 Background and Related Work

This section overviews inference attacks, encompassing their classifications and potential attack surfaces. Since there is a lack of research directly related to topology inference attacks on DFL, this paper examines topology inference studies conducted in other domains, including communication systems and social networks.

2.1 Inference Attacks

Inference attacks exploit ML models to extract sensitive information without direct access to the underlying data [Salem *et al.*, 2018]. By analyzing model behaviors or outputs, adversaries can infer properties of the data, model parameters, or system structure. As FL grows in adoption for its privacy-preserving capabilities, it also faces increased vulnerability to such attacks [Yin *et al.*, 2021]. Inference attacks vary in objectives and strategies, with common types including:

- **Membership Inference Attack:** Determines whether a specific data sample was part of the training dataset, often using shadow models or prediction confidence scores to differentiate between training and unseen data [Shokri *et al.*, 2017]. This is critical in sensitive domains like healthcare or finance.
- **Model Inversion Attack:** Reconstructs input data or infers its properties by iteratively optimizing inputs to match observed model outputs, posing risks in applications involving sensitive information like facial recognition or medical data [Fredrikson *et al.*, 2015].
- **Property Inference Attack:** Infers characteristics of the training data, such as demographic distributions, by analyzing model updates or outputs. In FL, this can involve monitoring node-specific behaviors to deduce shared properties of local datasets [Ganju *et al.*, 2018].
- **Attribute Inference Attack:** Targets specific attributes of training data, often by injecting malicious samples to influence the model’s learning process and make it vulnerable to data leakage [Gong and Liu, 2018].

These attacks not only compromise users’ sensitive information and undermine data security but also erode trust in FL’s privacy protection mechanisms. As a result, users may hesitate to participate in the training process, undermining the overall effectiveness of the FL system.

However, existing research on inference attacks in FL primarily focuses on CFL, with limited exploration of privacy leakage in DFL. Moreover, the critical role of DFL’s overlay topology has received insufficient attention in these studies.

2.2 Topology Inference

Topology inference is explored in various research domains, such as identifying source–destination paths in communication systems and uncovering interconnections among nodes in social networks.

Communication Systems

In communication systems, most protocols are designed to avoid ring formation, resulting in tree-like overlay topologies. Moreover, many topology inference studies commonly assume a single path between nodes [Castro *et al.*, 2004]. A

widely used approach involves leveraging ICMP-based protocols, such as the traceroute, to map network topologies effectively [Jin *et al.*, 2006]. Tomography-based metrics, like packet loss rates, further aid in deducing a system’s topology: by observing loss rates from a source node to a target node, one can estimate the likelihood of a direct connection and thereby reconstruct the network [Coates *et al.*, 2002]. Additionally, by measuring the timestamps of sent and received packets, it is possible to determine the number of forwarding hops, offering deeper insight into the overall network configuration [Hou *et al.*, 2020].

Social Networks

Social networks generally refer to the social structure formed by individuals in society connected by a specific relationship. In social networks, user interactions (e.g., likes, retweets) serve as valuable signals for topology modeling and inference by capturing how information diffuses across the network [Gomez-Rodriguez *et al.*, 2012]. However, this behavioral data is often incomplete, especially in large-scale settings, necessitating methods like noisy sparse subspace clustering to infer network structures from partial observations [Wang *et al.*, 2016]. Meanwhile, social networks are dynamic and time-sensitive, and they frequently exhibit small-world properties.[Gong *et al.*, 2012] incorporate these distributional patterns as prior knowledge in evolutionary models to better capture network changes over time.

Communication networks that often assume tree topologies and social networks are typically modeled as small-world networks; however, these assumptions do not hold for DFL network topologies. Moreover, common inference tools and metrics, such as traceroute, packet loss rate, or user interaction data, are not readily applicable in DFL contexts, creating the need for specialized inference metrics and strategies tailored to the particularities of DFL systems.

3 Overlay Topology in DFL

The overlay topology in DFL significantly affects model convergence. The overlay topology is modeled as an undirected graph $G = (V, E)$, where V is the set of nodes and E represents the edges indicating direct communication links between nodes. The adjacency matrix A encodes the graph structure, where:

$$A_{ij} = \begin{cases} 1 & \text{if nodes } i \text{ and } j \text{ are connected,} \\ 0 & \text{otherwise.} \end{cases} \quad (1)$$

The degree matrix D is a diagonal matrix where $D_{ii} = \text{degree}(i) + 1$. The aggregation process is governed by the normalized aggregation matrix:

$$P = D^{-1}(A + I), \quad (2)$$

where I is the identity matrix. This formulation ensures P is row-stochastic ($\sum_j P_{ij} = 1$), enabling consistent scaling during aggregation.

DFL proceeds iteratively over T rounds, comprising local training and model aggregation steps. Let $M_t = [\theta_1^{(t)}, \theta_2^{(t)}, \dots, \theta_N^{(t)}]$ represent the models of all nodes at round t , where $\theta_i^{(t)}$ denotes the parameters of node i .

During the training stage, each node updates its model using its local dataset:

$$M_t = \tilde{M}_{t-1} + \delta_t, \quad (3)$$

where δ_t represents local updates, and \tilde{M}_{t-1} is the aggregated model from round $t - 1$.

In the aggregation stage, nodes aggregate models from neighbors using the aggregation matrix P :

$$\tilde{M}_t = PM_{t-1}. \quad (4)$$

The model parameters after T rounds can be expressed as:

$$M_T = P^T M_0 + \sum_{t=1}^T P^{T-t} \delta_t. \quad (5)$$

Assuming G is connected (i.e., no isolated nodes), the spectral radius of P satisfies $\rho(P) < 1$. Additionally, under bounded local updates (e.g., using SGD or Adam), there exists $C > 0$ such that $\|\delta_i^{(t)}\| \leq C$ for all t and i . As T increases, the influence of the initial model diminishes:

$$\|P^T M_0\| \leq \|P^T\| \|M_0\| \rightarrow 0 \quad \text{as } T \rightarrow \infty. \quad (6)$$

The cumulative effect of local updates is:

$$\sum_{t=1}^T P^{T-t} \delta_t, \quad (7)$$

where $\|P^{T-t} \delta_t\|$ is bounded by $\|P^{T-t}\| \|\delta_t\|$. Since $\|P^{T-t}\| \rightarrow 0$ as $T \rightarrow \infty$, the impact of individual updates diminishes, and the series converges due to $\rho(P) < 1$.

Thus, it can be seen that the convergence behavior of DFL is influenced by the topology captured by P . Initially, the aggregation dynamics (powers of P) dominate, reducing the influence of M_0 . Over time, local updates drive the learning process, modulated by the decaying powers of P . This interplay underscores the importance of overlay topology in determining convergence efficiency and outcomes.

Given the critical role of overlay topology, it is essential to study potential information leakage through model updates and develop effective methods to protect sensitive topology information in DFL systems.

4 Problem Statement

Theoretical analysis of the DFL learning process reveals that overlay topology is crucial in determining system performance, robustness, and privacy. This section introduces the problem of topology inference and categorizes potential attack types based on the attacker's knowledge and capabilities.

Consider a DFL system represented by an undirected graph $G = (V, E)$, where V is the set of participating nodes, and E is the set of edges representing direct communication links between nodes. The adjacency matrix A of size $|V| \times |V|$ encodes the network topology, as defined in Equation (1).

An attacker aims to infer a predicted adjacency matrix A' that approximates the ground truth A as closely as possible, thereby revealing sensitive topology information.

The effectiveness of topology inference attacks depends on the attacker's knowledge and capabilities. The following assumptions are made. **(i) Internal Adversary:** The attacker is an internal participant in the DFL system and can identify a subset of nodes. **(ii) Decoupled Information:** Node-level information (e.g., models and datasets) and network-level information (e.g., connections) are treated as separate assets. For instance, an attacker may know a node's model but not its connections.

Let $V' \subset V$ represent a set of nodes known to the attacker and $E' \subset E$ represent the subset of edges known to the attacker, where $\emptyset \subsetneq E' \subsetneq E$ to represent partial knowledge. The attacker's goal is to infer the entire edge set E based on partial knowledge of V' and E' .

For each node $i \in V$, the local model is represented as M_i , and the local dataset is represented as D_i . This paper assumes that models and data within a node are distinct assets. Thus, the attacker's capabilities are defined as follows:

- **Model Knowledge:** The attacker can access models of known nodes V' , forming the set: $M' = \{M_i \mid i \in V'\}$.
- **Dataset Knowledge:** The attacker may not have access to the datasets D_i of these nodes. The datasets known to the attacker are denoted by: $D' \subseteq \{D_i \mid i \in V'\}$ or $D' = \emptyset$.

Based on the attacker's knowledge and capabilities, the topology inference attack is classified into five scenarios:

- **Scenario 1:** The attacker knows all node models and all the datasets, and only partial edge information ($M' = M, D' = D, \emptyset \subsetneq E' \subsetneq E$).
- **Scenario 2:** The attacker knows all node models and none of the datasets, and only partial edge information ($M' = M, D' = \emptyset, \emptyset \subsetneq E' \subsetneq E$).
- **Scenario 3:** The attacker knows all node models and all the datasets, but no edge information ($M' = M, D' = D, E' = \emptyset$).
- **Scenario 4:** The attacker knows all node models and none of the datasets, but no edge information ($M' = M, D' = \emptyset, E' = \emptyset$).
- **Scenario 5:** The attacker knows partial models and none of the datasets, but has no knowledge of the edges ($\emptyset \subsetneq M' \subsetneq M, D' = \emptyset, E' = \emptyset$).

For Scenario 1, since the attacker can control all nodes and knows partial information about the edges, it can be classified as a white-box attack. Scenarios 2, 3, and 4 can be categorized as gray-box attacks. For attack scenario 5, no information is available regarding the total number of nodes or edges, making it infeasible to fully reconstruct the network topology with the approaches considered. As a result, this work only considers the attack scenarios 1, 2, 3, and 4.

5 Topology Inference Attack

This section first explores the metrics that attackers can exploit to carry out topology inference attacks, and then designs attack strategies for various attack scenarios.

5.1 Attack Metrics

In a DFL system, attackers may leverage the local data and local models available at each known node. Additionally,

DFL’s decentralized communication mechanism allows attackers to access models transmitted from neighboring nodes. Thus, this paper proposes four attack metrics that attackers can exploit: relative loss, relative entropy, cosine similarity, and Euclidean similarity.

- **Relative Loss.** This metric evaluates how well a model trained on one node’s data generalizes to another node’s dataset. Consider a model f_i trained on node i ’s dataset D_i , and let D_j be the dataset of another node j . The relative loss $\text{Relative Loss}_{i,j}$ measures the performance of f_i on D_j . A lower relative loss indicates better transferability and generalization across nodes:

$$\text{Relative Loss}_{i,j} = \mathcal{L}(f_i, D_j) \quad (8)$$

where $\mathcal{L}(f, D)$ is the loss function used by the model f on dataset D .

- **Relative Entropy.** This metric measures the uncertainty of f_i ’s predictions on D_j . While relative loss focuses on correctness, relative entropy focuses on confidence. A model may be confident (low entropy) but still perform poorly if it is incorrect.

$$\text{Relative Entropy}_{i,j} = -\frac{1}{|D_j|} \sum_{x \in D_j} \sum_k y_k(x) \log(f_{i,k}(x)) \quad (9)$$

where $y_k(x)$ is the true label distribution for sample x and $f_{i,k}(x)$ is the predicted probability of class k under model f_i .

- **Cosine Similarity.** This metric compares the direction of two parameter vectors \mathbf{a} and \mathbf{b} derived from different models. If both vectors point in similar directions, their cosine similarity is high. In DFL, a high cosine similarity suggests that the two nodes frequently aggregate their parameters, resulting in more closely aligned models:

$$\text{Cosine Similarity}(\mathbf{a}, \mathbf{b}) = \frac{\mathbf{a} \cdot \mathbf{b}}{\|\mathbf{a}\| \|\mathbf{b}\|} \quad (10)$$

where $\mathbf{a} \cdot \mathbf{b}$ is the dot product, and $\|\mathbf{a}\|$, $\|\mathbf{b}\|$ are the L2 norms of the vectors \mathbf{a} and \mathbf{b} , respectively.

- **Euclidean Similarity.** It quantifies how similar two vectors are based on the Euclidean distance between them. A higher Euclidean similarity indicates that the two models are numerically closer, while a smaller distance suggests they differ significantly:

$$\text{Euclidean Similarity}(\mathbf{a}, \mathbf{b}) = \frac{1}{1 + \sqrt{\sum_{i=1}^n (a_i - b_i)^2}} \quad (11)$$

where a_i and b_i are the i -th elements of \mathbf{a} and \mathbf{b} .

Relative loss and entropy require the attacker to use both the local model and the local dataset, which are suitable for attack scenarios 1 and 3. In contrast, cosine similarity and Euclidean similarity depend solely on the models and do not require access to the datasets, which are suitable for attack scenarios 2 and 4.

5.2 Attack Strategies

The attacker’s objective in a topology inference attack is to construct a predicted adjacency matrix A' of size $|V| \times |V|$

Algorithm 1 Supervised Topology Inference Attack

Require: X : Attack metrics, Y^k : Known edges, Y^m : Missing edges, M : Attack model

Ensure: A' : Predicted adjacency matrix

```

1: function TOPOLOGYINFERENCE( $X, Y^k, Y^m$ )
2:    $D_{train} \leftarrow \text{EXTRACTNODEPAIRSANDLABELS}(X, Y^k)$ 
3:    $D_{test} \leftarrow \text{EXTRACTNODEPAIRS}(X, Y^m)$ 
4:    $M \leftarrow \text{InitializeSupervisedModel}()$ 
5:    $M.\text{train}(D_{train})$ 
6:    $Y'^m \leftarrow M.\text{predict}(D_{test})$ 
7:    $A' \leftarrow \text{COMBINE}(Y^k, Y'^m)$ 
8:   return  $A'$ 
9: function EXTRACTNODEPAIRSANDLABELS( $X, Y^k$ )
10:   $D_{train} \leftarrow []$ 
11:  for each  $(i, j)$  in  $Y^k$  do
12:     $D_{train}.\text{append}(\text{GetNodeMetrics}(X[i], X[j]), Y^k[i, j])$ 
13:  return  $D_{train}$ 
14: function EXTRACTNODEPAIRS( $X, Y^m$ )
15:   $D_{test} \leftarrow []$ 
16:  for each  $(i, j)$  in  $Y^m$  do
17:     $D_{test}.\text{append}(\text{GetNodeMetrics}(X[i], X[j]))$ 
18:  return  $D_{test}$ 

```

that closely approximates the ground-truth matrix. This can be viewed as a binary classification problem, determining whether each element A'_{ij} in A' equals one or zero.

Supervised Attack Strategy: In Attack Scenarios 1 and 2, since the attacker has knowledge of the true labels for some edges, a supervised classification approach is employed in this work to perform the attack. Given partial edges and their labels, these can be leveraged to train the attack model M . After training, M predicts the unknown edges to generate the predicted adjacency matrix A' , as shown in Algorithm 1.

Unsupervised Attack Strategy: For scenarios 3 and 4, where true labels are unavailable, this paper proposes an attack strategy based on unsupervised clustering, as shown in Algorithm 2. Since edges are known to fall into two categories, edge and non-edge group, the clustering algorithm M is configured for two clusters ($K = 2$). The attack metrics X are then clustered by M , producing a predicted adjacency matrix A' .

These attack algorithms enable the implementation of diverse strategies, tailored to varying levels of attacker knowledge and capabilities, to effectively infer the topology of the DFL.

6 Evaluation

This work empirically validates the effectiveness of the proposed topology inference attack. First, it identifies which metrics yield stronger attack performance. Building on these results, it then thoroughly evaluates the attack strategy under various conditions, including different datasets, topologies, node counts, and data preprocessing methods. This comprehensive assessment demonstrates the robustness and applicability of the proposed topology inference attack.

Algorithm 2 Unsupervised Topology Inference Attack

Require: X : Attack metrics, $K = 2$, M : Attack model**Ensure:** A' : Predicted adjacency matrix

```
1: function TOPOLOGYINFERENCE( $X$ )
2:    $g_1, g_2 \leftarrow$  CLUSTERNODEMETRICS( $X, K$ )
3:    $avg_1 \leftarrow$  CALCULATEMEAN( $g_1$ )
4:    $avg_2 \leftarrow$  CALCULATEMEAN( $g_2$ )
5:   if  $avg_1 < avg_2$  then
6:      $EdgeGroup \leftarrow g_1, NonEdgeGroup \leftarrow g_2$ 
7:   else
8:      $EdgeGroup \leftarrow g_2, NonEdgeGroup \leftarrow g_1$ 
9:    $A' \leftarrow$  CREATEADJACENCYMATRIX( $EdgeGroup$ )
10:  return  $A'$ 
11: function CLUSTERNODEMETRICS( $X, K$ )
12:   $M \leftarrow$  InitializeClusteringModel( $K$ )
13:  return  $M.fit(X)$ 
14: function CREATEADJACENCYMATRIX( $EdgeGroup$ )
15:  Initialize  $A'$  as a zero matrix
16:  for each pair  $(i, j)$  in  $EdgeGroup$  do
17:     $A'[i, j] \leftarrow 1$ 
18:  return  $A'$ 
```

6.1 Experimental Setups

This section describes the configurations employed in the experiments.

A. Dataset and Model: All experiments are conducted on three datasets: MNIST, Fashion-MNIST, and CIFAR10, widely used in ML and inference attack benchmarking.

- **MNIST [LeCun and Cortes, 2010]:** Contains 60,000 grayscale training images and 10,000 test images of handwritten digits (0–9) at 28×28 resolution. A two-hidden-layer MLP (256 and 128 neurons) trained with Adam ($lr=1e-3$) is used.
- **FMNIST [Xiao *et al.*, 2017]:** Similar size and format to MNIST, but with 10 categories of clothing items. A CNN with two convolutional layers (32 and 64 filters, kernel size 3×3), ReLU, and max-pooling is employed.
- **CIFAR10 [Krizhevsky *et al.*, 2009]:** Contains 60,000 32×32 RGB images from 10 categories. The training set is only treated with basic image normalization. The image pixel values are normalized to keep the original image content unchanged. A MobileNet [Sandler *et al.*, 2019] is used for the model training.

B. Topology Setting: All experiments employ a DFL network that includes five topologies: a ring, a star, and three Erdős-Rényi (ER) graphs with probabilities $p = 0.3$, $p = 0.5$, and $p = 0.7$ [Erdős *et al.*, 2012]. These configurations cover a spectrum of network densities, ranging from sparse to dense.

C. Federation Setting: All experiments employ the following DFL configurations:

- **Number of Nodes:** The network size is set to 10, 20, or 30 nodes, with training data randomly assigned to each node in an Independent and Identically Distributed (IID) manner, ensuring no overlap between nodes.
- **Total Rounds:** The total number of rounds is 10, 30, and 40 for networks with 10, 20, and 30 nodes, respectively.

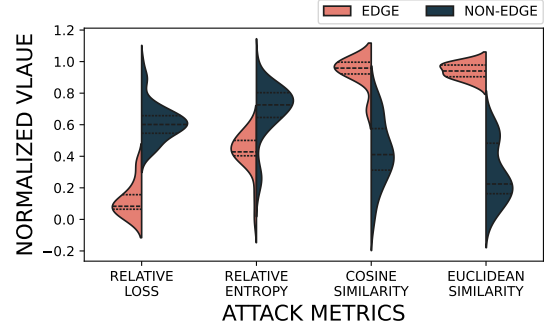


Figure 1: Normalized distributions of attack metrics in a 10-node ring-topology DFL system trained on the MNIST dataset. The “edge group” corresponds to metrics calculated between directly connected nodes, while the “non-edge group” corresponds to metrics calculated between nodes with no direct connection.

- **Local Epochs:** Two scenarios (3 and 10 local epochs) are considered to evaluate how varying levels of local overfitting affect the attack’s effectiveness.

D. Attack Models: The topology inference attack models are categorized by the attack strategy. For the **supervised attack strategy**, the models used are Logistic Regression [Wright, 1995], Support Vector Machine (SVM) [Hearst *et al.*, 1998], and Random Forest (RF) [Breiman, 2001]. For the **unsupervised attack strategy**, the models include K-Means [Lloyd, 1982], Gaussian Mixture Model (GMM) [Reynolds and others, 2009], and Spectral Clustering [Von Luxburg, 2007].

E. Evaluation Metric: Since the topology inference attack is formulated as a binary classification problem, the **F1-Score** set is used as the evaluation metric.

6.2 Selection of Attack Metrics

Selecting appropriate attack metrics is critical to the success of inference attacks. An effective attack metric should distinguish between connected and non-connected nodes as clearly as possible. To this end, the first part of this experiment examines the effectiveness of the four proposed attack metrics by analyzing their respective distributions. Figure 1 illustrates the distributions of these metrics for a 10-node ring topology DFL system trained on the MNIST dataset, comparing directly connected nodes (the edge group) with those not (the non-edge group). To facilitate direct comparison, all values have been normalized. The results indicate that the relative loss for connected nodes is notably lower than that for non-connected nodes, with minimal overlap between the respective distributions. By contrast, the relative entropy metric exhibits substantially greater overlap. Since computing the relative loss requires access to local models and data, it has been employed in attack scenarios 1 and 3.

Regarding similarity-based metrics, the Euclidean similarity between connected models is distinctly higher than that between non-connected models, displaying no overlap between the distributions. The cosine similarity, on the other

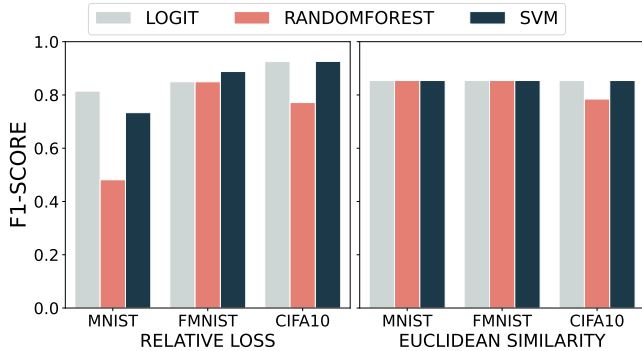


Figure 2: F1-Scores of three **supervised** attack models for topology inference attacks, using relative loss and Euclidean similarity on three datasets under a 10 nodes DFL system with ER 0.5 topology.

hand, shows a considerably more significant degree of overlap. Thus, the Euclidean similarity has been adopted as the attack metric in scenarios where only local models are available (attack scenarios 2 and 4).

6.3 Selection of Attack Models

Building on the attacker’s knowledge and capabilities, the topology inference attack is formulated either as a supervised learning problem (attack scenarios 1 and 2) or an unsupervised learning problem (attack scenarios 3 and 4). Corresponding attack algorithms are developed for each scenario. Using the established attack metrics, experiments are conducted on three datasets under a DFL system with an ER 0.5 topology, aiming to select the effective attack model.

Figure 2 compares the F1-Score of three supervised algorithms across the three datasets. The results demonstrate that the Logit algorithm consistently achieves strong and stable performance in both attack scenarios and on all three datasets. Therefore, the Logit algorithm is chosen for supervised attacks (attack scenarios 1 and 2).

Figure 3 presents the F1-Score of three unsupervised algorithms evaluated on the three datasets for attack scenarios 3 and 4. Among these methods, the K-Means algorithm delivers the best and most stable results, making it the algorithm of choice for unsupervised attacks (attack scenarios 3 and 4).

6.4 Attack Performance

After establishing the attack metrics and selecting the appropriate attack models, the proposed topology inference attacks were evaluated on three datasets, encompassing four attack scenarios and five types of topologies. The results in Table 1 indicate that the proposed methodology is highly effective. In a 10-node network, all four attack scenarios achieve an F1-Score exceeding 0.8, demonstrating that even with access restricted to public models, there is a high probability of successfully inferring the sensitive topology of a DFL system.

Generally, attack scenario 1 yields the highest attack success rate when the number of nodes equals 20 and 30 due to its access to the most information, including local models, data, and partial edge knowledge. Meanwhile, the performance in attack scenario 2 declines when local data are un-

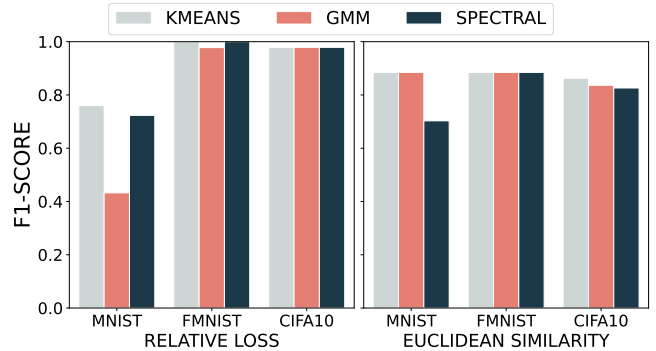


Figure 3: F1-Scores of three **unsupervised** attack models for topology inference attacks, using relative loss and Euclidean similarity on three datasets under a 10 nodes DFL system with ER 0.5 topology.

available, underscoring the critical importance of local data for accurate topology inference. Notably, attack scenario 3 also achieved a high attack success rate despite lacking edge information. This finding suggests that, compared to edge knowledge, access to local data contributes more to the successful inference of the topology in DFL. The complete set of experimental results is available in the supplementary materials.

A. Effect of Topology Density. To investigate the influence of topological characteristics on topology inference attacks, Figure 4 presents the F1-Scores achieved by attack scenario 1 and attack scenario 3 under five different topologies with 20 nodes (complete experimental results are provided in the supplementary materials). Among these, the star topology consistently achieves a high inference success rate. This is because each leaf node is connected solely to the central node in the star topology, thereby amplifying the differences in model parameters between leaf nodes and making the topology particularly easy to infer.

Additionally, under attack scenario 1, the inference performance negatively correlates with network density. In denser networks (such as ER 0.7), frequent information exchange between nodes reduces model heterogeneity, limiting the supervised attack model’s generalization and inference effectiveness. In contrast, network density does not adversely affect the unsupervised model.

B. Effect of Network Size. To evaluate the scalability of the proposed topology inference attacks, experiments were extended to networks comprising 20 and 30 nodes. The re-

Table 1: Topology inference attack performance on three datasets, encompassing four attack scenarios and five types of topologies.

NODES	DATASET	SC1	SC2	SC3	SC4
10	CIFAR10	0.922 ± 0.062	0.874 ± 0.033	0.989 ± 0.016	0.832 ± 0.099
	FMNIST	0.892 ± 0.109	0.885 ± 0.084	0.980 ± 0.044	0.849 ± 0.124
	MNIST	0.852 ± 0.096	0.899 ± 0.098	0.869 ± 0.087	0.849 ± 0.124
20	CIFAR10	0.877 ± 0.080	0.749 ± 0.068	0.843 ± 0.115	0.584 ± 0.166
	FMNIST	0.822 ± 0.115	0.769 ± 0.103	0.748 ± 0.151	0.607 ± 0.153
	MNIST	0.759 ± 0.126	0.712 ± 0.260	0.651 ± 0.178	0.698 ± 0.147
30	CIFAR10	0.815 ± 0.144	0.719 ± 0.155	0.800 ± 0.154	0.534 ± 0.213
	FMNIST	0.731 ± 0.156	0.787 ± 0.097	0.697 ± 0.183	0.604 ± 0.205
	MNIST	0.683 ± 0.148	0.809 ± 0.114	0.439 ± 0.134	0.615 ± 0.182

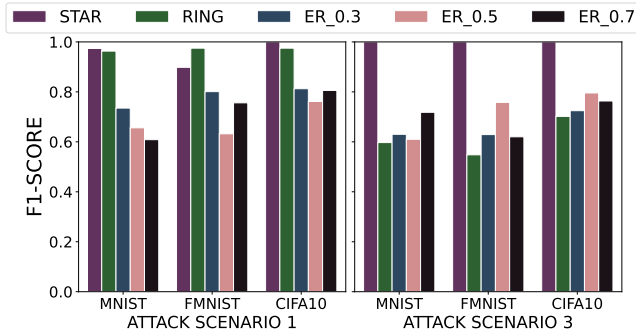


Figure 4: F1-Scores achieved by attack scenario 1 and attack scenario 3 under five different topologies with 10 nodes.

sults, summarized in Table 1, indicate that increasing the number of nodes generally makes the inference task more challenging, leading to a decline in attack performance. Nevertheless, under attack scenarios 1 and 2, F1-Scores consistently remain above 0.8 across all three datasets, demonstrating robust scalability. In contrast, attack scenario 4 exhibits a more pronounced decrease in performance as the network size increases.

7 Mitigation

The effectiveness of the proposed topology inference attacks indicates that topology in DFL systems can be discerned solely by analyzing model behaviors. This observation highlights the security and privacy concerns of DFL systems. This section proposes defense strategies to mitigate these vulnerabilities within DFL environments.

7.1 Reduce Overfitting

Similar to other inference attacks, the success of topology inference attacks also relies on the overfitting of the target model. To validate this, an experiment was conducted on a 10-node CIFAR10 network by increasing the number of local training epochs to induce greater overfitting. As shown in Figure 5, raising the local training epochs from 3 to 10 enhances the attack success rate under both attack scenario 1

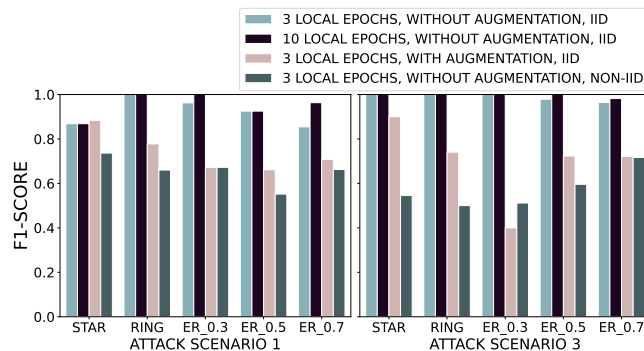


Figure 5: Impact of local training epochs, data augmentation, and data heterogeneity on the F1-Score of topology inference attacks in the CIFAR10 dataset.

and attack scenario 3 across all examined topologies. This result indicates that overfitting intensifies the risk of information leakage in DFL systems and suggests that mitigating overfitting can effectively mitigate topology inference attacks.

In line with this, data augmentation techniques were employed in the CIFAR10 dataset to mitigate overfitting. Specifically, each training image was randomly cropped by 4 pixels and padded. As depicted in Figure 5, introducing data augmentation substantially decreases the F1-Scores of the attacks across various topologies. Notably, for attack scenario 3 in the ER 0.5 network, the F1-score drops by as much as 50%. These results demonstrate that data augmentation not only enhances model generalization but also mitigates the risk of information leakage.

7.2 Data Heterogeneity

The distribution of data across nodes significantly influences the DFL model performance. Previous experiments have been conducted under the IID condition, where data is uniformly allocated across nodes. To explore the effects of data heterogeneity, specifically non-IID distributions, a Dirichlet distribution with a parameter of $\alpha = 0.1$ was utilized to simulate these non-IID conditions. Experiments were carried out using a CIFAR10 dataset distributed across 10 nodes, with the findings illustrated in Figure 5. The results indicate that an increase in data heterogeneity, achieved by setting the non-IID parameter $\alpha = 0.1$, significantly diminishes the effectiveness of topology inference attacks across all tested attack scenarios and network topologies. This outcome implies that enhancing data heterogeneity may serve as an effective strategy for reducing the risk of sensitive information exposure in DFL systems.

8 Conclusion and Future Work

This work introduces a novel topology inference attack against DFL, exposing critical vulnerabilities related to privacy and information leakage. By analyzing local models, attackers can accurately infer the overlay topology, one of DFL's most sensitive assets, highlighting the system's susceptibility to privacy breaches. The study explores various attack scenarios and develops tailored metrics, models, and algorithms, with experiments confirming the feasibility and effectiveness of these attacks.

Furthermore, factors like network size, density, model overfitting, and data heterogeneity significantly influence attack success. Mitigation strategies, such as data augmentation and increasing data heterogeneity, can enhance model generalization and reduce the risk of information leakage.

The present work focuses on attack scenarios 1 through 4 and does not yet address the most challenging attack scenario 5. Future research plans include exploring feasible strategies for Scenario 5, as well as extending the evaluations to a wider range of datasets.

References

[Beltrán *et al.*, 2024] Enrique Tomás Martínez Beltrán, Ángel Luis Perales Gómez, Chao Feng, Pedro

- Miguel Sánchez Sánchez, Sergio López Bernal, G r me Bovet, Manuel Gil P rez, Gregorio Mart nez P rez, and Alberto Huertas Celdr n. Fedstellar: A platform for decentralized federated learning. *Expert Systems with Applications*, 242:122861, 2024.
- [Beltr n *et al.*, 2023] Enrique Tom s Beltr n, Mario Quiles P rez, Pedro Miguel S nchez S nchez, Sergio L pez Bernal, G r me Bovet, Manuel Gil P rez, Gregorio Mart nez P rez, and Alberto Huertas Celdr n. Decentralized federated learning: Fundamentals, state of the art, frameworks, trends, and challenges. *IEEE Communications Surveys and Tutorials*, 25(4):2983–3013, 2023.
- [Breiman, 2001] Leo Breiman. Random forests. *Machine learning*, 45:5–32, 2001.
- [Castro *et al.*, 2004] Rui Castro, Mark Coates, Gang Liang, Robert Nowak, and Bin Yu. Network tomography: Recent developments. 2004.
- [Coates *et al.*, 2002] AHeroIII Coates, Alfred O Hero III, Robert Nowak, and Bin Yu. Internet tomography. *IEEE Signal processing magazine*, 19(3):47–65, 2002.
- [Dayal *et al.*, 2023] Saroj Dayal, Dima Alhadidi, Ali Abbasi Tadi, and Noman Mohammed. Comparative analysis of membership inference attacks in federated learning. In *Proceedings of the 27th International Database Engineered Applications Symposium*, pages 185–192, 2023.
- [Erd s *et al.*, 2012] L szl  Erd s, Antti Knowles, Horng-Tzer Yau, and Jun Yin. Spectral statistics of erd s-r nyi graphs ii: Eigenvalue spacing and the extreme eigenvalues. *Communications in Mathematical Physics*, 314(3):587–640, 2012.
- [Feng *et al.*, 2024] Chao Feng, Alberto Huertas Celdr n, Jan Von der Assen, Enrique Tom s Mart nez Beltr n, G r me Bovet, and Burkhard Stiller. Dart: A solution for decentralized federated learning model robustness analysis. *Arxiv*, page 100360, 2024.
- [Fredrikson *et al.*, 2015] Matt Fredrikson, Somesh Jha, and Thomas Ristenpart. Model inversion attacks that exploit confidence information and basic countermeasures. In *Proceedings of the 22nd ACM SIGSAC conference on computer and communications security*, pages 1322–1333, 2015.
- [Ganju *et al.*, 2018] Karan Ganju, Qi Wang, Wei Yang, Carl A Gunter, and Nikita Borisov. Property inference attacks on fully connected neural networks using permutation invariant representations. In *Proceedings of the 2018 ACM SIGSAC conference on computer and communications security*, pages 619–633, 2018.
- [Gomez-Rodriguez *et al.*, 2012] Manuel Gomez-Rodriguez, Jure Leskovec, and Andreas Krause. Inferring networks of diffusion and influence. *ACM Transactions on Knowledge Discovery from Data (TKDD)*, 5(4):1–37, 2012.
- [Gong and Liu, 2018] Neil Zhenqiang Gong and Bin Liu. Attribute inference attacks in online social networks. *ACM Transactions on Privacy and Security (TOPS)*, 21(1):1–30, 2018.
- [Gong *et al.*, 2012] Neil Zhenqiang Gong, Wenchang Xu, Ling Huang, Prateek Mittal, Emil Stefanov, Vyas Sekar, and Dawn Song. Evolution of social-attribute networks: measurements, modeling, and implications using google+. In *Proceedings of the 2012 internet measurement conference*, pages 131–144, 2012.
- [Hearst *et al.*, 1998] Marti A. Hearst, Susan T Dumais, Edgar Osuna, John Platt, and Bernhard Scholkopf. Support vector machines. *IEEE Intelligent Systems and their applications*, 13(4):18–28, 1998.
- [Hou *et al.*, 2020] Tao Hou, Zhe Qu, Tao Wang, Zhuo Lu, and Yao Liu. Proto: Proactive topology obfuscation against adversarial network topology inference. In *IEEE INFOCOM 2020-IEEE Conference on Computer Communications*, pages 1598–1607. IEEE, 2020.
- [Hu *et al.*, 2022] Hongsheng Hu, Zoran Salcic, Lichao Sun, Gillian Dobbie, Philip S Yu, and Xuyun Zhang. Membership inference attacks on machine learning: A survey. *ACM Computing Surveys (CSUR)*, 54(11s):1–37, 2022.
- [Jin *et al.*, 2006] Xing Jin, W-P Ken Yiu, S-H Gary Chan, and Yajun Wang. Network topology inference based on end-to-end measurements. *IEEE Journal on Selected areas in Communications*, 24(12):2182–2195, 2006.
- [Krizhevsky *et al.*, 2009] Alex Krizhevsky, Geoffrey Hinton, et al. Learning multiple layers of features from tiny images. 2009.
- [LeCun and Cortes, 2010] Y. LeCun and C. Cortes. MNIST handwritten digit database. <http://yann.lecun.com/exdb/mnist/>, 2010. Accessed: 2016-01-14.
- [Lloyd, 1982] Stuart P. Lloyd. Least squares quantization in pcm. *IEEE Transactions on Information Theory*, 28(2):129–137, 1982. Originally presented as a Bell Labs Technical Report in 1957.
- [McMahan *et al.*, 2017] Brendan McMahan, Eider Moore, Daniel Ramage, Seth Hampson, and Blaise Aguera y Arcas. Communication-efficient learning of deep networks from decentralized data. In *Artificial intelligence and statistics*, pages 1273–1282. PMLR, 2017.
- [Reynolds and others, 2009] Douglas A Reynolds et al. Gaussian mixture models. *Encyclopedia of biometrics*, 741(659-663), 2009.
- [Salem *et al.*, 2018] Ahmed Salem, Yang Zhang, Mathias Humbert, Pascal Berrang, Mario Fritz, and Michael Backes. MI-leaks: Model and data independent membership inference attacks and defenses on machine learning models. *arXiv preprint arXiv:1806.01246*, 2018.
- [Sandler *et al.*, 2019] Mark Sandler, Andrew Howard, Menglong Zhu, Andrey Zhmoginov, and Liang-Chieh Chen. Mobilenetv2: Inverted residuals and linear bottlenecks, 2019.
- [Shokri *et al.*, 2017] Reza Shokri, Marco Stronati, Congzheng Song, and Vitaly Shmatikov. Membership inference attacks against machine learning models. In *2017 IEEE Symposium on Security and Privacy (SP)*, pages 3–18, 2017.

- [Von Luxburg, 2007] Ulrike Von Luxburg. A tutorial on spectral clustering. *Statistics and computing*, 17:395–416, 2007.
- [Wang *et al.*, 2016] Yining Wang, Yu-Xiang Wang, and Aarti Singh. Graph connectivity in noisy sparse subspace clustering. In *Artificial Intelligence and Statistics*, pages 538–546. PMLR, 2016.
- [Wright, 1995] Raymond E Wright. Logistic regression. 1995.
- [Xiao *et al.*, 2017] H. Xiao, K. Rasul, and R. Vollgraf. Fashion-mnist: A novel image dataset for benchmarking machine learning algorithms. *arXiv:1708.07747 [cs, stat]*, September 2017. Accessed: 2023-07-11.
- [Yin *et al.*, 2021] Xuefei Yin, Yanming Zhu, and Jiankun Hu. A comprehensive survey of privacy-preserving federated learning: A taxonomy, review, and future directions. *ACM Computing Surveys (CSUR)*, 54(6):1–36, 2021.